UNIVERSITY OF CALIFORNIA

Santa Barbara

New middle Cambrian hyolith genus and species and echinoderm ossicles from the Georgina Basin, Australia

A Thesis submitted in partial satisfaction of the

requirements for the degree Master of Science

in Geological Sciences

by

Miranda M. Stripe

Committee in charge:

Professor Susannah Porter, Chair

Professor Andre Wyss

Professor David Lea

September 2015

The thesis of Miranda M. Stripe is approved.

_____

Andre Wyss

_____

David Lea

_____

Susannah Porter, Committee Chair

September 2015

New middle Cambrian hyolith genus and species and echinoderm ossicles from the Georgina Basin, Australia

ACKNOWLEDGEMENTS

This project was made possible by the Earth Research Institute and the National Science Foundation (EAR-1411594). Thanks to S. Porter and team who collected these samples. Thanks also to committee members S. Porter, A. Wyss, and D. Lea for their invaluable help in improving the quality and content of this paper. Thanks to T. Harman and A. Fuentes for assisting with fossil isolation. Special thanks to J. Moore, who went above and beyond the role of friend and colleague in providing guidance and critique on this study and document.

ABSTRACT

New middle Cambrian hyolith genus and species and echinoderm ossicles from the Georgina Basin, Australia

by

Miranda M. Stripe

The study herein describes a new genus and species of orthothecid hyolith and numerous echinoderm ossicles. The internal mold of the hyolith bears an apical ridge and is of uniform width, distinguishing it from other known hyoliths. Biological significance of its internal apical structure is unclear, though hypotheses proposed include a streamlining effect and presence of a terminal spine on the original shell. Inclusion of the supposed *Circotheca stylus* depicted in Dzik (1980: fig. 7) into this species expands the newly described hyolith's geographic range to Baltica and extends its temporal occurrence into the Late Cambrian. Some of the ossicles resemble echinoderm taxa (e.g., stylophorans and eocrinoids), but many ossicle morphologies share little to no similarities to known Cambrian echinoderms. Several fragmented ossicles bear phosphatic casts around their pores similar to *Cantabria labyrinthica* remains. Such results suggest that *C. labyrinthica* may represent echinoderm ossicles, not lobopodian plates as originally proposed by Clausen and Álvaro (2006).

Introduction

Small shelly fossils (SSFs), typically phosphatic or secondarily phosphatized, occur globally throughout the Cambrian (Matthews and Missarzhevsky, 1975; Dzik, 1994), providing invaluable data for understanding early metazoan life. The exceptional detail in SSFs is attributed to the phosphatization taphonomic window, an interval in which phosphate replaced original (skeletal) material, allowing for the preservation of organisms whose original mineralogy may not have lasted over such extensive time (Runnegar, 1985; Dzik, 1994; Brasier, 1990; Xiao and Schiffbauer, 2009; Porter, 2004a; Creveling et al., 2014). For example, many mollusc and hyolith species possess aragonitic shells, which would likely have recrystallized to calcite over geologic time due to aragonite's thermodynamic instability under low pressures (Brown et al., 1962; Zeebe and Wolf-Gladrow, 2001). Microstructural details often lost in recrystallization to calcite are replicated via phosphatization. To preserve the original shell microstructure in phosphatic casts, apatite must first nucleate on the original calcium carbonate (Kasioptas et al., 2008). Thus, apatite pseudomorphosis occurs along phosphatic (internal) molds (Runnegar, 1985; Feng and Sun, 2003), mimicking the original microstructure instead of forming spatially independent crystals (Ames, 1959; Putnis, 2002). Well preserved microstructure can potentially be used to determine taxonomic affinities (e.g., Runnegar, 1985; Kouchinsky, 2000; Porter, 2008; Moore and Porter, in prep.). Additionally, apatite replacement permits easier fossil extraction from calcareous rocks via maceration in acetic acid. This allows for three-dimensional examination of SSFs as opposed to limited examination in thin section.

Macerated SSF residues document the presence of numerous extant (e.g., molluscs, brachiopods, and echinoderms) and extinct (e.g., halkieriids, chancelloriids, and hyoliths)

taxa throughout the Cambrian. Many of these extinct taxa do not fit clearly into modern groups due to insufficient data for phylogenetic placement. Further investigation of these specimens and their associated assemblages will increase understanding of these extinct groups and their relations to modern taxa. The exceptional preservation of microstructure in SSFs makes such endeavors possible.

The SSFs examined herein derive from the Beetle Creek Formation in the Georgina Basin, Australia. Previously studied components of this assemblage include halkieriids (Porter, 2004b), bradoriids (e.g., Fleming, 1973; Hinz-Schallreuter, 1993; Jones and Kruse, 2009), palaeoscolecid worms (Müller and Hinz-Schallreuter, 1993), echinoderms (Clausen et al., 2009), hyoliths (Kruse, 2002), and trilobites (Öpik, 1979). This study describes two additional taxa from this assemblage: tubular fossils representing a new species of hyolith, and net-like fossils showing a wide array of echinoderm ossicle morphologies.

Geologic Setting

Fossils examined in this study were collected in the Georgina Basin, Australia – a 325,000-km^2 intracratonic depression spanning regions of the Northern Territory and western Queensland (Shergold and Druce, 1980). As part of the Centralian Superbasin that resulted from the breakup of Rodinia in the Neoproterozoic (Walter et al., 1995; Lindsay, 2002), the Georgina Basin formed from crustal extension during the late Proterozoic (Lindsay et al., 1987; Southgate and Shergold, 1991), and contains sedimentary and volcanic fill of Neoproterozoic to Devonian age (Kruse, 2002). The samples under consideration here derive from the Beetle Creek Formation at Rogers Ridge in Queensland; this unit, middle Cambrian in age, contains well-preserved phosphatized fossils (e.g., Fleming, 1973; Runnegar and Jell,

1976; Shergold and Southgate, 1986; Southgate et al., 1988; Müller and Hinz, 1992; Kruse, 1998; Porter, 2004b). At the Rogers Ridge locality, the Beetle Creek Formation disconformably overlies the Thorntonia Limestone; it is overlain, with a conformable to laterally disconformable contact, by the organic-rich Inca Shale (Müller and Hinz-Schallreuter, 1993).

The Beetle Creek Formation consists of the lower Siltstone Member and the upper Monastery Creek Phosphorite Member. The Siltstone Member is 50–60-m thick and contains chert, white fissile siltstone, and some pelletal phosphorite, while the upper portion of the formation is composed of 10–15-m thick grainstone phosphorite, phosphatic and siliceous siltstone, chert, sandstone, shale, and phosphatic limestone (de Keyser and Cook, 1972; Soundry and Southgate, 1989). The fossils analyzed in this study were derived from tabular, fine-grained limestone of the Monastery Creek Phosphorite Member, which was originally deposited below fair-weather wave base (Porter, 2004b). The Monastery Creek Phosphorite Member contains the agnostoid arthropod *Ptychagnostus gibbus*, which indicates the late Templetonian and Floran Stages (~505 Ma; Series 3, Stage 5) of the middle Cambrian of Australia (Öpik et al., 1957; Öpik, 1979; Geyer and Shergold, 2000; Peng et al., 2012). During the Cambrian, this locality was situated near 20°N (Eldridge et al., 1997; Brock et al., 2000) on a marine shelf (Russell and Trueman, 1971). Evidence for a marine setting is further supported by myriad marine specimens (e.g., brachiopods, halkieriid sclerites, and trilobites) recovered from the samples (PK98-39, PK98-41, PK98-42, PK98-44, PK98-45, and PK98-48) within this study.

Materials and Methods

Fossils were extracted from calcareous rocks using a 10–15% acetic acid solution. Samples were picked through by hand to isolate fossils from macerated residues.

The fossils were mounted on stubs using a light microscope. Stubs, sputter-coated with a 16–22-nm thick carbon layer, were examined with a FEI Quanta 400f field-emission, environmental scanning electron microscope under high vacuum at 5–20 kV and 6.5–19.0 mm working distance.

Systematic Paleontology

?Phylum MOLLUSCA Cuvier, 1797

Class HYOLITHA Marek, 1963

Order ORTHOTHECIDA Marek, 1966

Family INCERTAE

Remarks – The hyolith species described below does not clearly belong to a currently recognized orthothecid family. It most closely compares to members of Circothecidae in that it possesses a circular transverse section (a character which is rather variable within this family; Missarzhevsky, 1969). Erection of Family Circothecidae was based on genus *Circotheca* (Syssoiev, 1968), described to have a straight-cut aperture (Missarzhevsky, 1969). However, Missarzhevsky (1969) also described curving growth lines on *Circotheca*, which reflect the aperture's shape (Berg-Madsen and Malinky, 1999). Therefore, contrary to Missarzhevsky's (1969) assertion, *Circotheca*'s aperture is not planar, but instead bears a "short, ligula-like projection" (Berg-Madsen and Malinky, 1999). The possible growth lines

(Figs. 1H, 3E) on the specimens herein lack such curvature, ruling out both *Circotheca* and Circothecidae as possible taxonomic groups to which the hyolith species belongs.

Genus NEWGENUS new genus

Type species – Newgenus newspecies by monotypy

Diagnosis – As for type species by monotypy.

NEWGENUS NEWSPECIES new species

?1980 *Circotheca stylus*; Dzik, p. 230, fig.7

?2002 Indeterminate hyolith; Kruse, fig. 5d,e

Holotype – PK98-42A31 (Fig. 2)

Diagnosis – Relatively straight conchs with circular cross-sections showing little to no widening in diameter aperturally. Conch's internal mold bears a point, connecting to a dorsal ridge ranging from 20–80 μm in length. Apertures are flat and lack a ligula.

Occurrence – Middle Cambrian (Late Templetonian/Floran; Series 3) Monastery Creek Phosphorite Member, Beetle Creek Formation, Rogers Ridge, Burke River Outlier, western Queensland, Australia.

Description – Conchs are tubular, ranging from 200–900 μm in length, with circular cross-sections 35–145 μm in diameter. Most are uniformly wide (95 μm on average; SD=13.5 μm; count=119 specimens) along their entire length, although a few specimens bear ~2 μm bulges

on their dorsal faces (Fig. 1B). Specimens show little or no curvature through most of their long axis, but curve more strongly dorsally near the apex (Figs. 2–5). A narrow ridge (20–80 μm in length) runs longitudinally down the dorsal side of the apex, typically ending where the conch begins to curve slightly inward on the dorsal face of the internal mold (Figs. 1C,J, 2C). On some specimens, the ridge's end (i.e., where the conch bends) gives the apex a triangular appearance (Figs. 1B–D, 3E, 4E,G, 5D), while the ridge is less dramatic and forms a more bulbous apex in other specimens (Figs. 1A,E,G,I,K, 2A, 3B,F,J, 4A). Faint growth lines(?), visible as lines on some internal molds, lie parallel to the straight aperture (Figs. 1H, 3E). Complete specimens with smooth-rimmed apertures bear no (ventral) ligula (Fig. 3A–D, F–J). Some specimens have transverse rod-shaped to fibrous structures (~0.5 μm wide), perpendicular to the long axis of the shell and parallel to the shell's surface (Fig. 1F,L). However, some specimens show evidence for multiple fibrous layers at oblique angels to one another (Fig. 4C,F,H).

Materials – More than one hundred specimens from samples PK98-39, -41, -42, -44, -45, and -48.

Preservation – The fossils are preserved as phosphatic internal molds composed of randomly oriented, sub-micrometric, equant apatite crystals (*cf.* Xiao and Schiffbauer, 2009: fig. 6; Figs. 3D, 4D). Pronounced tubular structures run along the surface of some specimens (Fig. 5A–E), representing borings of cyanobacteria (Runnegar, 1985). Some molds bear partial casts of the shell wall due to replacement by apatite crystals. The rod-shaped to fibrous structures that lie perpendicular to the long axis of the shell are typical of lamello-fibrillar microstructure seen in many hyoliths (Moore and Porter, in prep), representing the interior shell surface or lamina within the innermost portion of the shell wall. The fibrous nature of

these structures suggest that the original mineralogy was aragonitic, consistent with the mineralogy of other hyoliths (e.g., Marek and Yochelson, 1976; Kouchinsky, 2000; Malinky et al., 2004; Porter, 2010).

Remarks – The specimen is considered an orthothecid hyolith primarily based on its straight-cut aperture and lack of a ventral ligula. The hyolith's prominent apical ridge and uniform width distinguish it from other orthothecids. The apex of several species of hyoliths, including one occurring in the material examined (Fig. 5F), is pointed (e.g., *Decoritheca excavata* Holm, 1893; *Microcornus eximius* Duan, 1984; *Recilites* Marek, 1967), but none bear the ridge observed in the new hyolith species.

The biological significance of this ridge is unclear, but it and the narrow shell width may have reduced resistance when the animal traveled across the substrate. However, the small size of the hyolith likely restricted it to the laminar flow portion of the water column, rendering such a streamlined shell unavailing unless in a high-energy environment. No casts are complete enough to demonstrate that the conch's outer ornamentation mirrored that of the inner surface. Yet the Cambrian mollusc *Aldanella attleborensis* bears a mucro on the apex of its shell similar to that of the hyolith herein, where the cast of its shell shows the same structure as the internal mold (Dzik and Mazurek, 2013). Therefore, it is reasonable to presume that the hyolith's outer ornamentation resembles the structure of its internal mold. Assuming this streamline hypothesis is true, the two species' apical ridges must have evolved for different purposes (if any) as *A. attleborensis* would not benefit from a turbulence-reducing ridge in the center of its highly-coiled shell. Thus, the streamline hypothesis seems unlikely as their shared apical structures are absent in other Cambrian SSFs.

Another potential explanation for the internal mold's ridge could be the presence of a spine on the original shell's apex, which might not occur on the internal mold. Such a structural dynamic is analogous to a banana, where the fruit (like the internal mold) has a round to somewhat triangular tip and the unpeeled banana (comparable to the hyolith conch) has a prominent stem (or spine). Considering that the apical portion of the conch is larval, perhaps an apical spine aided in hatching, ripping the egg capsule (assuming a composition similar to that of modern gastropods).

Within the new hyolith species, the apex varies from bulbous to more (tri)angular. The diagnostic ridge, in conjunction with slight conch curvature, likely contributes to the emphasized angular nature of the apex. This difference in morphology is not considered a sufficient basis for erecting two different species, but rather is considered plastic variation within the species. For example, specimens with a more highly curved conch may have grown more quickly ventrally during development, causing the dorsal side to curve. This development would likely be reflected in shell growth lines (Fretter and Pilkington, 1971), though definitive growth lines are not present in the specimens herein. Alternatively, degree of curvature may vary depending on the size of the larval shell at the time of metamorphosis (*cf.* Dzik, 1978). During larval development, ridge growth could potentially continue, terminating when adult shell growth begins. In this scenario, differences in ridge length would contribute to degree of apical curvature, accounting for the variation in apical shapes.

The new hyolith species is considered to (questionably) include both an unidentified hyolith mentioned in Kruse (2002: fig. 5d,e) and a specimen assigned by Dzik (1980: fig. 7) to *Circotheca stylus* (Holm, 1983). Both these hyoliths have similar lengths and pointed apices to those of the hyolith herein. The conchs also possess faint growth lines (if actually

present) as well as relatively straight-cut, longitudinally perpendicular apertures. However, the hyolith illustrated in Kruse (2002), also from the Monastery Creek Phosphorite Member at Rogers Ridge, may only bear a pointed apex rather than possessing a ridge-like feature (it is difficult to determine based on the figure alone), and its flat aperture is not clearly at a 90° angle to the shell's longitudinal axis. The apex of *C. stylus* from Dzik (1980) more closely resembles that of the hyolith herein than does the mucro of the indeterminate hyolith in Kruse (2002). The indeterminate hyolith's pointed apex appears to run straight with the dorsal face of the specimen, while most of the new hyoliths' conchs curve dorsally near the apex (e.g., Fig. 1B) as does that of *C. stylus* depicted in Dzik (1980).

Though the *C. stylus* described in Dzik (1980: fig. 7) has affinities to the hyolith herein, the species as a whole is not included in the new hyolith species as the specimen in Dzik (1980) is mistakenly placed in *C. stylus* (Holm, 1893). This assertion is based on comparisons of growth lines and apical shape. The faint growth lines visible on the specimen in Dzik (1980) lie perpendicular to the long axis of the conch, showing no curvature toward the aperture on the ventral surface. Such convex curves are present in *Circotheca stylus* as defined by Holm (1893). As mentioned previously, this convexity rules out a straight-cut aperture; instead, the *Circotheca* conch bears a ligula-like shelf (Berg-Madsen and Malinky, 1999). The specimen in Dzik (1980) has a broken aperture, yet its straight growth lines suggest it lacks a ligula-like projection. Addtionally, *C. styla* (which includes *C. stylus*, Dzik, 1980) figured in Berg-Madsen and Malinky (1999: fig. 9) have broken apices, though the conchs appear to narrow to what would be a small tip as opposed to the bulbous or triangular apex seen in Dzik (1980) and the specimens herein. Therefore, *C. stylus* illustrated in Dzik

(1980) is excluded from *Circotheca* and tentatively placed within the hyolith species described herein.

If the specimen illustrated in Dzik (1980), which was attributed to *C. stylus* (Holm, 1893), is indeed a representative of the new hyolith species, then this would expand the geographic and stratigraphic range of the newly described hyolith. The specimen is from an erratic boulder (E-278) recovered in Międzyzdroje, Western Pomerania, Poland, estimated to be early Late Cambrian in age by the presence of the conodont *Westergaardodina tricuspidata* Müller, 1959 (Dzik, 1980). In addition to the specimen attributed to *C. stylus*, the assemblage from the erratic boulder includes eocrinoids, bradoriids, brachiopods, *Pelagiella*, and other hyoliths (Dzik, 1980) – an assemblage similar to that from the Monastery Creek Phosphorite Member. If the specimen does represent a member of the new hyolith species, this would suggest a broad geographic range for the species, as the entirety of Gondwana is thought to have been located between the two localities (Australia, which was part of Eastern Gondwana, and Baltica) during the Late Cambrian (Scotese et al., 1979; Bambach et al., 1980; Berg-Madsen, 1987) and, to a lesser extent, in the middle Cambrian (Eldridge et al., 1997; Brock et al., 2000). One might therefore expect that this hyolith might be found elsewhere between Australia and Baltica. However, Berg-Madsen (1987) discussed the similarities between two geographically-isolated fauna, the middle Cambrian Bornholm and New Zealand assemblages, attributing these similarities to their comparable latitudes (45°S vs. 45°N, respectively) and environments. Yet Międzyzdroje and western Queensland did not lie at similar latitudes (45°S vs. 20°N) during the middle Cambrian (Brock et al., 2000) nor during the Late Cambrian (Berg-Madsen, 1987). Though this assemblage was deposited elsewhere before transported glacially to Międzyzdroje, it likely did not travel far

as many erratic boulders from northern Germany contain conodonts (e.g., *Westergaardodina* sp.) similar to those found in the Late Cambrian of Sweden (Müller, 1971), suggesting that such erratic boulders from nearby Międzyzdroje also originated from Sweden. Consistent with this, reconstructed flowline patterns in Overweel (1997) illustrate that the glacier that deposited erratic boulder E-278 originated from Sweden. Therefore, inclusion of the *C. stylus* specimen depicted in Dzik (1980) would expand the geologic distribution of the new hyolith species, suggesting possible occurrence elsewhere along the Gondwanan coast, and extending the existence of the hyolith into the Late Cambrian.

Phylum ECHINODERMATA Klein, 1734

ECHINODERM OSSICLES

Material – Hundreds of echinoderm ossicles and fragments from the Monastery Creek Phosphorite Member, Beetle Creek Formation, Georgina Basin, Australia (samples PK98-41, -42, -44, -45, and -48).

Description – Net-like molds of stereom with smooth surfaces that border trabecula-shaped voids <5–10 μm in diameter (Fig. 6D). Original calcitic material presumably occupied these voids (before acetic acid maceration), wrapping around diagenetically filled circular to subcircular pores (10–50 μm in diameter) that were once empty spaces in the original specimen. Some of the pore spaces are oblong, appearing almost as if two round pores fused together (Fig. 6A). Most specimens bear labyrinthic or laminar stereom as defined in Smith (1980), though microstructure varies as does overall morphology; these are described below.

Preservation – Ossicles are preserved as external phosphatic molds. Smooth surfaces are interpreted to represent the contact between the external mold and the outer surface of the

original trabeculae prior to maceration (Fig. 6D). Diagenetic apatite occupies the pores of the stereom and rests on some of the smooth surfaces (Figs. 6D, 7A–C). However, some material may represent partial replacement of the original calcite by apatite (Figs. 6H, 7B?). These round crystallites compose a thin layer on the smooth surfaces (Fig. 6H), seeming to have formed on the surfaces as opposed to merely be resting on them. In some specimens, portions of the mold surround the entire trabecular void, manifesting as a granular to smooth, bumpy covering (Fig. 6).

Original skeletal material is thought to be calcareous based on the following observations: (1) distinct, consistent network of trabecular-shaped voids (Figs. 6, 7, 8A,B), and (2) smooth surfaces encompassing those voids (Fig. 6D,E). The network of tubes suggests that skeletal material originally occupied these voids, a conclusion supported by the characteristically smooth walls of the tubes where the original material likely contacted the diagenetic apatite remaining after maceration.

Remarks – These net-like fossils superficially resemble *Cantabria labyrinthica*, an oval-shaped fossil composed of meshwork microstructure and calcium phosphate from the early middle Cambrian of the Cantabrian Mountains (Clausen and Álvaro, 2006). Based on the fossils' consistently thick-walled (original?), bilayered, calcium phosphate hollow tubes and the lack of phosphatization of echinoderm ossicles within the same samples, Clausen and Álvaro (2006) concluded that *C. labyrinthica* is not an echinoderm but instead potentially represents lobopodian plates similar to those of *Microdictyon*. Some fragments herein resemble *C. labyrinthica*, possessing hollow tubes consisting of layers of apatite (Fig. 7B,D). However, some of these specimens also bear distinct smooth-walled components – representing the outer surfaces of trabeculae – along the side of the tubes (i.e., original pore

spaces), on which the apatite layers are partially formed (Fig. 7A–E). Additionally, Clausen and Álvaro (2006) characterized *C. labyrinthica* by its subcircular overall morphology and trapezoidal cross-section, neither of which can be seen in the fossils herein due to their fragmentary nature.

This evidence does not exclude referral of these particular specimens to *C. labyrinthica*, but it may suggest that *C. labyrintica* is an echinoderm. Elicki (2011) contended that *C. labyrintica* is not a lobopodian plate based on its similarities to echinoderm stereom (i.e., identical internal ultrastructure) and on the "weak" arguments by Clausen and Álvaro (2006) for non-echinoderm relations. Additionally, Clausen and Álvaro (2006) describe perforations that connect neighboring phosphatic tubes. If *C. labyrinthica* specimens in Clausen and Álvaro (2006) were preserved as partially replaced trabeculae (i.e., the outermost portions of trabeculae), or as diagenetic calcium phosphate coatings, and lacked large amounts of filling by diagenetic material within trabecular voids, then the tubes and their connecting perforations in *C. labyrinthica* could constitute galleried stereom described in Smith (1980). Alternatively, the meshwork microstructure of *C. labyrinthica* could represent the phosphatic mold of irregular perforate stereom, a conclusion fortified by the cross-sectional images depicted in Clausen and Álvaro (2006). In both cases, *C. labyrinthica* may indeed represent partially phosphatized echinoderm ossicles, not lobopodian plates.

The assertion that the net-like fragments, both those with and without *C. labyrinthica* similarities, represent echinoderm ossicles is further supported by the wide array of their morphologies (described below). In particular, basals and columnals occur in the assemblage, both morphotypes having the microstructure mentioned above (Fig. 8), typical of previously

described echinoderms from the middle Cambrian (e.g., Clausen and Smith, 2008; Clausen et al., 2009; Elicki, 2011**)**.

Though echinoderm ossicles from the Monastery Creek Phosphorite Member (e.g., Smith and Jell, 1990; Clausen et al., 2009; Zamora et al., 2010) and other Cambrian (Series 3) assemblages (e.g., Clausen and Smith, 2005; Clausen and Smith, 2008; Domke and Dornbos, 2010; Elicki, 2011; Clausen and Peel, 2012) have previously been described, the samples studied herein contain several morphotypes unexplored by other authors. For example, numerous spines occur within this assemblage, yet are scarce in Cambrian literature (e.g., Berg-Madsen, 1986; Clausen and Peel, 2012). Though several morphotypes can be (questionably) assigned to their respective groups, some of the ossicles described below do not clearly belong to any known group of (Cambrian) echinoderms or are too fragmented to confidently place. Most notable are the fin- and fan-shaped morphotypes – ossicle shapes foreign to the current literature on Cambrian echinoderms. Therefore, classification beyond Echinodermata for some morphotypes is not attempted.

ECHINODERM OSSICLE MORPHOTYPES

BASALS

Type A (Fig. 9A)

Description – Round, flat base with five irregular small notches along its edge and a short, cylindrical structure stemming off its center. The cylindrical structure caves in toward its center. Stereom type is indeterminate due to excess diagenetic coating.

Remarks – This individual resembles the second basal morphotype described in Clausen et al. (2009: fig. 7L) and Zamora et al. (2010: fig. 4E), possessing a circular base with a concave

proximal face. Unlike the specimen in Clausen et al. (2009), the basal described here shows no evidence for three rounded notches on the proximal face, though absence of such could be attributed to poorer preservation of this particular specimen. However, the specimen may truly lack such notches, in which case it bears closer resemblance to that in Zamora et al. (2010: fig. 4D). The irregular notches in the base portion of the ossicle likely resulted from chipping, thus not representing a true anatomical feature.

Type B (Fig. 9B)

Description – Round, flat base with a short, three-dimensional rectangular structure stemming off its center, and labyrinthic stereom.

Remarks – If indeed a basal, the corresponding columnals would likely be thin and rectangular. This presumably would not be very sturdy, though such an arrangement would increase the surface area to volume ratio (SA:V). Crinoids and pelmatozoans feed using brachioles (not absorbing food through their columnals), so increasing this ratio poses no obvious advantage in terms of obtaining nutrients; however, it could aid in thermoregulation, though such a use is not particularly useful for a relatively sessile echinoderm. Considering the structural quality of the presumed corresponding columnals and minimal-to-no gain with increased SA:V, this ossicle may instead have represented a surface plate with a notch on it.

Type C (Fig. 9C)

Description – Oblong flat base with a short, narrow, cylindrical structure (fragmented?) stemming off its center. Stereom is labyrinthic.

Remarks – The term “basal” is used loosely here, as the proximal face may be fragmented. If broken, the cylindrical structure could be longer than that typical of echinoderm holdfasts. In

that case, the ossicle could represent a different anatomical portion such as a spiny thecal plate (*cf.* Clausen and Peel, 2012: fig. 18h,l).

BOX-SHAPED (Fig. 9D)

Description – Flat, rectangular face with shorter rectangular components rising in the same direction on all edges of the base, forming a box-shaped structure. Whether the entire specimen is completely boxed-in is unclear due to (possible) fragmentation. All three specimens possess labyrinthic stereom.

Remarks – This morphotype does not clearly represent a specific group of echinoderm. Other box-like ossicles have been described by some authors (e.g., Clausen and Smith, 2008), but, unlike the ossicles herein, these have an inner core of fascicular stereom. It is possible that the box-shaped fossils described here are fragmentary and do not represent the ossicles' true overall shapes.

BRANCHING

Type A (Fig. 9E)

Description – One thick and two thinner cylindrical branches stemming off a single point, with the largest angle between the two thinner branches. The terminal portions of each branch appear broken. Between one thin branch and the thick branch is a flat piece of stereom, forming a right angle across from the end of the thin branch. Ossicle possesses labyrinthic stereom.

Remarks – This morphotype does not closely resemble any described disarticulated Cambrian echinoderm ossicle. However, Sumrall et al. (1997) depicts thecal plates of a Late

Cambrian echinoderm, *Tatonkacystis codyensis*, to which the ossicle herein could belong, representing a bulged out portion on a single plate. In this case, the flat projection between two branches would represent the non-bulging portion of the thecal plate.

The ossicles are also similar to those that compose gogiid brachioles. One particular middle Cambrian specimen, *Sinoeocrinus globus*, illustrated by Lin et al. (2008), bears brachioles that fork near their tips. The ossicle described above could fit such a junction, thus representing a gogiid like *S. globus*. However, gogiid brachioles typically have food grooves – a feature not seen in the ossicle herein, though food grooves could be on the surface opposite that visible in Fig. 9E.

Yet another possibility is that the ossicle represents a fragment of a stylophoran marginal plate. Such a marginal plate is illustrated in Ubaghs and Robison (1988) and Sumrall et al. (1997), where the ossicle would represent the M1 plate of *Scotiaecystis*? spp. (*cf.* Sumrall et al., 1997: figs. 6.3, 8) or the M5 plate of a cornute stylophoran like *Archaeocothurnus goshutensis* (*cf.* Sumrall et al., 1997: figs. 4.3, 6.2) or *Corthunocystis*? *bifuda* (*cf.* Ubaghs and Robison, 1988: figs. 4, 5.1, 6.3). However, the resemblance of the ossicle herein to the aforementioned stylophorans is largely based on illustrations, though the figured specimen of *A. goshutensis* does clearly show the M5 plate that the ossicle could represent. Definitive placement of this ossicle may be possible with additional, better preserved material.

Type B (Fig. 9F)

Description – Cylindrical ossicle bearing labyrinthic stereom, with an infilled inner core. One end of the cylinder has a branching component, where one side curves upward, connecting to

the flat surface of the cylinder. This projection forms a smooth, oblique angle with the long axis of the cylinder, giving the branch a triangular shape.

Remarks – This branching ossicle is reminiscent of long, laterally concave columnals (e.g., Clausen and Smith, 2008; Clausen and Peel, 2012; Zamora et al., 2013). However, the projection at one end of the cylinder precludes its classification as a columnal, leaving this morphotype unassigned to a specific echinoderm group.

CANAL (Fig. 9G)

Description – Rectangular surface with a half-cylinder structure forming a canal through its center. Stereom is labyrinthic.

Remarks – This ossicle resembles various brachitaxial, uniserial appendages from several middle Cambrian assemblages in that it has an overall square to rectangular shape, bisected by a semi-cylindrical groove (e.g., Clausen et al., 2009; Clausen and Peel, 2012; Zamora et al., 2013). However, the ossicle herein only has one distinct canal, while specimens described by other authors (except that in Clausen and Peel (2012), whose canal face appears eroded) bear smaller concavities adjacent to the central groove. Though the ossicles vary slightly, the ossicle herein likely represents a component of a brachial arm.

?COLUMNAL

Type A (Fig. 9H)

Description – Rectangular face with an oblong cross-section, connected to a short, broad cylindrical stump. The entire ossicle bears labyrinthic stereom.

Remarks – This ‘columnal’ is overall cylindrical like those described in other studies (e.g., Clausen et al., 2009), yet its stacked-cup appearance distinguishes it from even those that lack a consistent circumference in that it narrows abruptly. Thus, this ossicle is very tentatively considered a columnal as it bears no close resemblance to other known columnals except in its overall cylindrical shape.

Type B (Fig. 9I,J)

Description – Discoidal overall morphology with a hollowed-out center and labyrinthic stereom. One specimen (Fig. 9I) widens slightly and gradually on the far disk-shaped side, giving a sloping effect to the outer edge of the disk.

Remarks – These ossicles share similarities in their overall shape to columnals depicted in Berg-Madsen (1986), Clausen et al. (2009), and Clausen and Peel (2012). The ossicles herein, however, differ from those in Clausen et al. (2009) in that they lack notches around their narrower hollow center. The ‘columnal’ with asymmetrical bases may actually be a discoidal holdfast like that in Clausen and Peel (2012), suggesting that the other two could also represent holdfasts. Yet Clausen and Peel (2012) also depict a holomeric columnal (type B) that fans out in the middle, in which case the ossicle herein would represent the innermost portion of such a columnal. However, the holomeric columnals in Clausen and Peel (2012) bear fasicular stereom, unlike the labyrinthic stereom observed herein. A middle Cambrian ossicle depicted in Berg-Madsen (1986) also shows widening in its center, giving it an appearance analogous to an old-fashioned donut, but possesses the labyrinthic stereom consistent with the ossicles described here. Thus, the ossicles herein could be such columnals considering the rough edges along their circumference.

CUP-SHAPED (Fig. 9K)

Description – Short, cylindrical component with a concave base and labyrinthic stereom.

Remarks – The specimen does not resemble any described Cambrian echinoderm. If fragmented on the non-concave side, then it could potentially represent a spine like those described below. However, the thickness of the area around the concavity is narrower in this specimen than those seen in the spines. Additionally, the spines display evidence for galleried stereom, while the cup-shaped ossicle bears labyrinthic stereom.

FAN-SHAPED

Type A (Fig. 9L,M)

Description – Rectangular face with trabecular grooves (covered by diagenetic material) that run parallel to the long edge of the ossicle. One specimen has a rounded base extending off its rectangular portion (Fig. 9M). The other ossicle's rectangular component is longer, at the base of which a concaved structure branches perpendicularly to its rectangular surface (Fig. 9L). Both show evidence for fascicular stereom, though the latter may bear labyrinthic stereom at its base.

Remarks – The two ossicles within this morphotype are grouped based on their sole similarity of a rectangular face with grooved structures. The echinoderm taxon to which they belong is unclear, as is the case for most of the fan-shaped ossicles. However, the longer ossicle with the branching arched structure could potentially represent a spinal or digital process like that seen in *Cothurnocystis*? *bifida* (*cf.* Ubaghs and Robison, 1988). Still, the ossicle herein is much smaller than that described by Ubaghs and Robison (1988), having a

more rectangular shape than the serrated-blade morphology of the *Cothurnocystis*? *bifida* ossicle.

Type B (Fig. 9N)

Description – A grooved surface consisting of a slender, cylindrical stem smoothly connecting to a narrow fanning structure. This entire portion has a flat, rectangular component stemming off of it on one side.

Remarks – The overall shape of this ossicle does not resemble any known Cambrian ossicle.

Type C (Fig. 9O)

Description – A grooved, rectangular surface that narrows and attaches to a circular component that lies nearly perpendicular to the flat, rectangular surface. The ossicles bear fascicular stereom.

Remarks – The discoidal components of these rectangular ossicles suggest that the round portions may have attached to the main body of the echinoderm, while the rectangular portions projected off the organism. Such a structure could serve as a paddle to move the organism or potentially function as some sort of feeding structure. However, this is merely speculative as the true nature of these ossicles is unknown. Like the other fan-shaped morphotypes, similar ossicles have not been described in the Cambrian echinoderm literature.

Type D (Fig. 9P)

Description – A long, subcircular, flat ossicle with a flat, rectangular edge on one side and labyrinthic stereom. A cylindrical stem is inconspicuous on one side of the rectangular edge. Faint radial structures spread out from the cylindrical component.

Remarks – Considering the cylindrical structure and radial components, these ossicles may represent distal processes that stem off the main body of the echinoderm. However, the ossicles' taxonomic affinities are unclear and the nature of these ossicles cannot be definitively assessed.

FIN-SHAPED (Figs. 6A,B, 9Q,R)

Description – Round, flat surface attached to a long, slender branch. Some specimens have a branched portion nearly as wide as the flat surface's diameter. Stereom is labyrinthic in the rounded portion and becomes fascicular through the stemmed component.

Remarks – Like many of the fan-shaped ossicles, these fin-shaped ossicles do not clearly belong to a specific group of echinoderms. However, they share similarities to the digital process of the *Cothurnocystis*? *bifida* illustrated in Ubaghs and Robison (1988: fig. 4).

FRAGMENTS (Figs.6E–H, 7)

Description – Any pieces of ossicle-like material, i.e., bears the stereom microstructure described above (Fig. 8). Most fragments are flat. Stereom types include labyrinthic (most abundant), laminar, and retiform.

Remarks – These fragments cannot definitively be placed in any specific echinoderm group, though some could potentially be surface plates of various echinoderms. However, such an assessment is rather superficial as the only uniting characters are their relatively flat morphology and ubiquitous microstructure.

PETAL-SHAPED (Fig. 9S)

Description – Large, oval-shaped, flat surface that is connected by a flat edge, near which it smoothly indents and then widens again. Stereom is labyrinthic.

Remarks – This ossicle is much larger than the other ossicles described herein, though its taxonomic affinities are also unclear.

SPINES (Fig. 9T,U)

Description – Series of long, slender, parallel rods that bush out in tiers, narrowing down into a point at the tip of the spine. Some specimens come off a large, basal structure (Fig. 9T), while others have concave components in a cylindrical base no wider than the bottom bundle of slender components (Fig. 9U). The regular arrangement of the rods suggests galleried stereom, though the fanned out bases on some individuals is labyrinthic.

Remarks – The echinoderm to which these spines belong is unknown, though they possibly projected off the main body of the echinoderm, similar to the spines of sea urchins. The concave base in most of these spines may have served as a junction site for a ball-like appendage, acting as a ball-and-socket joint. The ball component likely sat down into a base like that seen in Fig. 9T. Modern sea urchin spines differ from these in that the urchin spine bears the ball appendage, attaching into a socket on the main body (e.g., *cf.* Märkel and Röser, 1983; Grossman and Nebelsick, 2013).

The spines herein also differ from other Cambrian spines or plates with spine-like projections. The overall morphology of the spine-in-base structure looks like the middle Cambrian thecal plate depicted in Clausen and Peel (2012: fig. 19FG), but the tiered structure seen in the spine is not visible in the thecal plate. Like the base of the spines, the thecal plates

have labyrinthic stereom (Clausen and Peel, 2012); however, the thecal plates possess this stereom throughout while the spines have galleried stereom above their base. Berg-Madsen (1986: fig. 4D) also described a spine-like ossicle from the middle Cambrian. Both this spine and the one herein have a concave base, yet the one in Berg-Madsen (1986) is notably different in that it widens from base to tip, where the top of the spine is flat. Also, the spine in Berg-Madsen (1986) has rod-like structures in grooves within the spine. Though the spines herein have rod-like structures, these rods result from phosphatic coating of the original stereom rather than fillings (diagenetic or original) of grooves in the stereom itself.

SQUARED DIVIDE (Fig. 9V)

Description – Square surface with a smaller rectangular component branching off perpendicularly near the center of the square component, which is slightly concave at this junction. One of the two specimens has another rectangular component, smooth and oblong in cross-section, stemming off the square component.

Remarks –The angular nature of these ossicles is reminiscent of edrioasteroid ambulacral plates (*cf.* Clausen and Peel, 2012: fig.11). However, ambulacral plates have two to three nearly parallel prongs, while the ossicles herein have two to four projections more or less perpendicular to one another.

STEMMED CANAL

Type A (Fig. 9W,X)

Description – Circular to subcircular base with a hollow, half-cylinder rising from the base. There is a subsequent rounded ‘canal’ from this arrangement. One specimen displays a flat

top (relative to the base), while the other two are fragmented and overall structure cannot be asserted. Specimens with visible microstructure bear galleried stereom.

Remarks – One of the ossicles (Fig. 9X), more fragmentary than the others, resembles the stylocone depicted in Clausen and Smith (2005: fig. 3a). Whether the other ossicles represent stylocones is doubtful as they flatten out into a base where the canal widens, unlike the stylocone in Clausen and Smith (2005).

Type B (Figs. 6C,D, 9Y)

Description – Semi-circular base with a hollow center. A rectangular component rises off this, bearing a rounded top. Whether the canal continues into the rectangular projection is unclear. Stereom is galleried in the rectangular portion and labyrinthic in the base.

Remarks – One of these ossicles (Fig. 6C) very closely resembles a spinal process of *Cothurncystis*? *bifida* (*cf.* Ubaghs and Robison, 1988: fig. 7.1). Thus, this ossicle is considered to be part of a stylophoran skeleton. However, the other ossicle of this morphotype has a more bulged-out base (Fig. 9Y), calling into question its affinities with stylophoran spinal processes.

Discussion

The Monastery Creek Phosphorite assemblage contains a plethora of well-preserved specimens that enables detailed descriptions like those herein. For example, the hyoliths possess complete apices, regarded as taxonomically significant by Jiang (1984), with detailed structures like the ridge seen in the new hyolith species. Echinoderm ossicles bear partial crystalline casts similar to the phosphatic tubes seen in *Cantabria labyrinthica* (Clausen and Álvaro, 2006), suggesting echinoderm affinities for the species. The new hyolith species also

bears partial casts, displaying layers of fibrous, oblique rods (Fig. 5) characteristic of the lamello-fibrillar microstructure seen in other hyoliths (e.g., Kouchinsky, 2000; Moore and Porter, in prep.).

Other than the hyolith described herein, only three other hyoliths appear in this assemblage. Among these are a possible hyolithomorph, a conical hyolith, and an unidentified hyolith (Fig. 5F). Despite this low diversity, tens to hundreds of the new hyolith species appear in each sample. Two hypotheses could account for this observation. For one, these specimens could represent juvenile hyoliths that died simultaneously (e.g., via an influx of anoxic water) before they could disperse. If true, then the samples collectively would represent a short span of time (on the order of days), or multiple mass deaths occurred throughout Stage 5 in this marine environment. Alternatively, the hyolith thrived in its environment, outcompeting other hyolith species with similar niches. Hyolithids and orthothecids are likely deposit-feeders (e.g., Runnegar et al., 1975; Marek and Yochelson, 1976; Babcock, 1988; Kruse, 1997; Devaere et al., 2014), so one species dominating others with similar feeding habits is not unreasonable.

Unlike the hyoliths from these samples, echinoderm ossicles show substantial morphological diversity. Though several ossicles likely belong within the same echinoderm clade, this assemblage contains more disparity than that described previously from the Monastery Creek Phosphorite Member (e.g., Clausen et al., 2009; Zamora et al., 2010). Echinoderm diversity within Australian Stage 5 was considered relatively low (Zamora et al., 2013: fig. 13.8a), but evidence herein suggests occurrence of at least two additional clades – eocrinoids (i.e., gogiids) and stylophorans. Studies like Clausen and Peel (2012) described echinoderm ossicles rivaling the morphological diversity depicted herein, yet several

morphotypes (e.g., fan-shaped ossicles) still elude placement within any known echinoderm clade.

Conclusion

The hyolith specimen discussed herein represents a new genus and species of orthothecid. Its prominent apical ridge and uniform width are unlike any other Cambrian hyolith, though an unidentified hyolith in Kruse (2002: fig. 5d,e) and a specimen erroneously assigned to *Circotheca stylus* by Dzik (1980: fig. 7) may also belong to the species. The latter hyolith's inclusion into the new hyolith species would indicate a wide geographic range for the species and extend its temporal range into the Late Cambrian.

The numerous echinoderm ossicles described in this study belong to several clades, including gogiids, pelmatozoans, and stylophorans. However, many ossicles show no clear affinities to known echinoderm taxa. Further investigation of the Monastery Creek Phosphorite Member and other middle Cambrian assemblages is needed to determine the echinoderms to which these ossicles belong.

Literature Cited

Ames, L.L. Jr. (1959). The genesis of carbonate apatites. *Economic Geology*, 56: 826–841.

Babcock, L.E. and R.A. Robison (1988). Taxonomy and Paleobiology of some Middle Cambrian *Scenella* (Cnidaria) and Hyolithidis (Mollusca) from Western North America. *University of Kansas Paleontological Contributions*, Paper 121: 1–22.

Bambach, R.K., C.R. Scotese, and A.M. Ziegler (1980). Before Pangea: The Geographies of the Paleozoic World. *American Scientist*, 68 (1): 26–38.

Berg-Madsen, V. (1986). Middle Cambrian cystoid (*sensu lato*) stem columnals from Bornholm, Denmark. *Lethaia*, 19: 67–80.

Berg-Madsen, V. (1987). *Tuarangia* from Bornholm (Denmark) and similarities in Baltoscandian and Australasian late Middle Cambrian faunas. *Alcheringa: An Australasian Journal of Palaeontology*, 11 (3): 245–259

Berg-Madsen, V. and J.M. Malinky (1999). A revision of Holm's late Mid and Late Cambrian hyoliths of Sweden. *Palaeontology*, 42 (5): 841–885.

Brasier, M.D. (1990). Phosphogenic events and skeletal preservation across the Precambrian-Cambrian boundary interval. *In* Notholt, A.J.G., and Jarvis, I., eds., Phosphorite Research and Development: Geological Society of London Special Publication No. 52, p. 289–303.

Brown, W.H., W.S. Fvfe, and F.J. Turner (1962). Aragonite in California glaucophane schists, and the kinetics of the aragonite-calcite transformation. *Journal of Petrology*, 3: 566–582.

Brock, G.A. and B.J. Cooper (1993). Shelly Fossils from the Early Cambrian (Toyonian) Wirrealpa, Aroona Creek, and Ramsay Limestones of South Australia. *Journal of Paleontology*, 67: 758–787.

Brock, G.A., M.J. Engelbretsen, J.B. Jago, P.D. Kruse, J.R. Laurie, J.H. Shergold, G.R. Shi, and J.E. Sorauf (2000). Paleobiogeographic affinities of Australian Cambrian faunas. *Memoir of the Association of Australasian Palaeontologists*, 23: 1–61.

Clausen, S. and J.J. Álvaro (2006). Skeletonized microfossils from the Lower–Middle Cambrian transition of the Cantabrian Mountains, northern Spain. *Acta Palaeontologica Polonica* 51 (2): 223–238.

Clausen, S. and J.S. Peel (2012). Middle Cambrian echinoderm remains from the Henson Gletscher Formation of North Greenland. *GFF*, 134 (3): 173–200.

Clausen, S. and A.B. Smith (2005). Paleoanatomy and biological affinities of a Cambrian deuterostome (Stylophora). *Nature*, 438: 351–354.

Clausen, S. and A.B. Smith (2008). Stem structure and evolution in the earliest pelmatozoan echinoderms. *Journal of Palaeontology*, 82 (4): 737–748.

Clausen, S., P.A. Jell, X. Legrain, and A.B. Smith (2009). Pelmatozoan arms from the Middle Cambrian of Australia: bridging the gap between brachioles and brachials? *Lethaia*, 42: 283–296.

Creveling, J.R., A.H. Knoll, and D.T. Johnston (2014). Taphonomy of Cambrian small shelly fossils. *PALAIOS*, 29 (6): 265–308.

Cuvier, G. (1797). *Tableau élementaire de l'histoire naturelle des animaux.* Baudouin, Paris, 710 pp.

De Keyser, F. and P.J. Cook (1972). Geology of the Middle Cambrian phosphorites and associated sediments of northwestern Queensland. *Bureau of Mineral Resources Geology and Geophysics Bulletin (Australia)*, 138, 79 p.

Devaere, L., S. Clausen, J.J. Álvaro, J.S. Peel, and D. Vachard (2014). Terreneuvian Orthothecid (Hyolitha) Digestive Tracts from Northern Montagne Noire, France; Taphonomic, Ontogenetic and Phylogenetic Implications. PLoS ONE 9 (2): 1–91.

Domke, K.L. and S.Q. Dornbos (2010). Paleoecology of the middle Cambrian edrioasteroid echinoderm *Totiglobus*: implications for unusual Cambrian morphologies. *PALAIOS*, 25: 209–214.

Duan, C.H. (1984). Small shelly fossils from the Lower Cambrian Xihaoping Formation in the Shennongjia District, Hubei Province—hyoliths and fossil skeletons of unknown affinities [in Chinese with English summary]. *Bulletin of the Tianjin Institute of Geology and Mineral Resources*, 7: 143–188.

Dzik, J. (1978). Larval development of hyolithids. *Lethaia*, 11: 293–299.

Dzik, J. (1980). Ontogeny of *Batrotheca* and related hyoliths. *Geologiska Föreningens i Stockholm Förhandlinger*, 102 (3): 223–233.

Dzik, J. (1994). Evolution of 'small shelly fossils' assemblages of the Early Paleozoic. *Acta Palaeontologica Polonica*, 39 (3): 247–313.

Dzik, J. and D. Mazurek (2013). Affinities of the alleged earliest Cambrian gastropod *Aldanella*. *Can. J. Zool.*, 91: 914–923.

Eldridge, J., D. Walsh, and C.R. Scotese (1997). *Plate Tracker for Windows 95 version 1*. CD-Rom.

Elicki, O. (2011). First skeletal microfauna from the Cambrian Series 3 of the Jordan Rift Valley (Middle East). *Memoirs of the Association of Australasian Palaeontologists*, 42: 153–173.

Feng, W. and W. Sun (2003). Phosphate replicated and replaced microstructure of molluscan shells from the earliest Cambrian of China. *Acta Palaeontologica Polonica* 48 (1): 21–30.

Fleming, P.J.G. (1973). Bradoriids from the *Xystridura* zone of the Georgina Basin, Queensland. *Geological Survey of Queensland Publication 356, Palaeontological Papers*, 31: 1–9.

Fretter, V. and M.C. Pilkington (1971). The larval shell of some Prosobranch gastropods. *J.M. B. Ass. U. K.*, 52: 49–62.

Grossman, J.N. and J.H. Nebelsick (2013). Comparative morphological and structural analysis of selected cidaroid and camarodont sea urchin spines. *Zoomorphology*, 132: 301–315.

Geyer, G. and J. Shergold (2000). The quest for internationally recognized divisions of Cambrian time. Episodes, 23:188–196.

Hinz-Schallreuter, I. (1993). Ostracodes from the Middle Cambrian of Australia. *Neues Jahrbuch für Geologie und Paläontologie, Abhandlungen,* 188: 305–326.

Holm, G. (1893). Sveriges kambrisk-siluriska Hyolithidae och Conulariidae. *Sveriges Geologiska Undersökning C*, 112: 1–170.

Jiang, Z. (1984). Evolution of early shelly metazoans and basic characteristics of Meishucun fauna. *Professional Papers of Stratigraphy and Palaeonotology*, 13: 1–22.

Jones, P.J. and P.D. Kruse (2009). New Middle Cambrian bradoriids (Arthropoda) from the Georgina Basin, central Australia. *Memoirs of the Association of Australasian Palaeontologists*, 37: 55–86.

Kasioptas, A., C. Perdikouri, C.V. Putnis, and A. Putnis (2008). Pseudomorphic remplacment of single calcium carbonate crystals by polycrystalline apatite. *Mineralogical Magazine*, 72 (1): 77–80.

Klein, J.T. (1734). *Naturalis dispositio Echinodermatum. Accessit lucubratiuncula de aculeis Echinorum marinorum, cum spicilegio de Belemnitis*. Schreiber, Gedani (Gdansk), 79 pp.

Kouchinsky, A. (2000). Skeletal microstructures of hyoliths from the Early Cambrian of Siberia. *Alcheringa: An Australasian Journal of Palaeontology*, 24 (2): 65–81.

Kruse, P.D. (1997). Hyolith guts in the Cambrian of northern Australia – turning hyolithomorphs upside down. *Lethaia*, 29: 213–217.

Kruse, P.D. (1998). *Cambrian palaeontology of the eastern Wiso and western Georgina basins*. Northern Territory Geological Survey Report, 9, 68 p.

Kruse, P.D. (2002). Biostratigraphic potential of Middle Cambrian hyoliths from the eastern Georgina Basin. *Alcheringa: An Australasian Journal of Palaeontology*, 26 (3): 353–398.

Lin, J., W.I. Ausich, Y. Zhao, and J. Peng (2008). Taphonomy, paleoecological implications, and colouration of Cambrian gogiid echinoderms from Guizhou Province, China. *Geol. Mag.*, 145 (1): 17–36.

Lindsay, J.F. (2002). Supersequences, superbasins, supercontinents – evidence from the Neoproterozoic–Early Palaeozoic basins of central Australia. *Basin Research*, 14: 207–223

Lindsay, J. F., J. Korsch, and R. Wilford (1987). Timing the breakup of a Proterozoic supercontinent: evidence from Australian intracratonic basins. *Geology*, 15: 1061–1064.

Malinky, J.M., M.A. Wilson, L.E. Holmer, and H. Lardeux (2004). Tubeshaped *incertae sedis*. In *The Great Ordovician Biodiversification Event* (eds. Webby B.D., F. Paris, M.L. Droser, I.G. Percival). Columbia University Press, New York, pp. 214–222.

Marek, L. (1963). New knowledge on the morphology of *Hyolithes*. Sborník geologickych ved, Rada Paleontologie, 1: 53–73.

Marek, L. (1966). Nové rody hyolitu z Ceského Ordoviku. *Časopis Národního Muzea, oddíl prírodovedny*, 135(2): 89–92.

Marek, L. (1967). The class Hyolitha in the Caradoc of Bohemia. *Sbornik geologickych ved, Řada Paleontologie*, 9: 51–113.

Marek, L. and E.L. Yochelson (1976). Aspects of the biology of the Hyolitha (Mollusca). *Lethaia*, 9: 65–82.

Märkel, K. and U. Röser (1983). The Spine Tissue in the Echinoid *Eucidaris tribuloides*. *Zoomorphology*, 103: 25–41.

Matthews, S.C. and V.V. Missarzhevsky (1975). Small shelly fossils of late Precambrian and early Cambrian age, a review of recent work. *Journal of the Geological Society* (London), 131: 289–304.

Missarzhevsky, V.V. (1969). Descriptions of hyoliths, gastropods, hyolithelminths, camenids, and forms of an obscure systematic position. 105–175. *In* Rozanov, A.Yu., V.V. Missarzhevsky, N.A.Volkova, L.G. Voronova, I.N. Krylov, B.M. Keller, I.K. Korolyuk, K. Lendzion, R. Michniak, N.G. Pykhova, and A.D. Sidorov. Tommotsky jarus i problema nizhnej granitzy Kembriya. Akademia Nauk SSSR. *Ordena Trudvogo krasnogo znameni Geologicheskij Institut, Trudy*, 206. [In Russian, English translation, 1981. *Paleontologic part*, 112–160. *In* Raben, M. E. (ed.). *The Tommotian Stage and the Cambrian Lower Boundary Problem*. Amerind, New Delhi, 359 pp.].

Moore, J.L. and S.M. Porter (in prep.). Shell microstructure of Cambrian hyolithomorph hyoliths.

Müller, K.J. (1959). Kambrische Conodonten. *Zeitschrift der Deutschen Geologischen Gesellschaft*, 111 (2): 434–485.

Müller, K.J. (1971). Cambrian Conodont Faunas. Cambrian conodont faunas. In *Symposium on Conodont Biostratigraphy*, Sweet, W. C. and S.M. Bergström eds, *Geological Society of America Memoir*, 127: 5–20.

Müller, K.J. and I. Hinz (1992). Cambrogeorginidae fam. nov., soft integumented Problematica from the Middle Cambrian of Australia. *Alcheringa: An Australasian Journal of Palaeontology*, 16: 333–353.

Müller, K.J. and I. Hinz-Schallreuter (1993). Palaeoscolecid worms from the Middle Cambrian of Australia. *Palaeontology*, 36: 549–592.

Öpik, A.A (1979). Middle Cambrian agnostids: systematics and biostratigraphy. *Bureau of Mineral Resources Bulletin (Geology and Geophysics, Australia)*, 172, 188 p.

Öpik, A.A., M.R. Banks, J.N. Casey, B. Daily, J. Gilbert-Tomlinson, L.C. Noakes, L.P. Singleton, D.E. Thomas, and D.M. Traves (1957). The Cambrian geology of Australia. *Bureau of Mineral Resources Bulletin (Geology and Geophysics, Australia)*, 49, 284 p.

Overweel, C.J. (1977). Distribution and transport of Fennoscandinavian indicators. *Scripta Geologica*, 43: 1–117.

Parkhaev, P.Y. and Y.E. Demidenko (2010). Zooproblematica and Mollusca from the Lower Cambrian Meishucun Section (Yunnan, China) and Taxonomy and Systematics of the Cambrian Small Shelly Fossils of China. *Paleontological Journal*, 44 (8): 883–1161.

Peng, S.C., L.E. Babcock, and R.A. Cooper (2012). The Cambrian Period, 451–502. In Gradstein, F.M., and J.G. Ogg, M. Schmitz, and G.J. Ogg (eds) *The Geologic Time* Scale, 2012. Elsevier, Boston.

Porter, S.M. (2004a). Closing the Phosphatization Window: Testing for the Influence of Taphonomic Megabias on the Pattern of Small Shelly Fossil Decline. *PALAIOS*, 19: 178–183.

Porter, S.M. (2004b). Halkieriids in Middle Cambrian Phosphatic Limestones from Australia. *Journal of Paleontology*, 78 (3): 574–590.

Porter, S.M. (2008). Skeletal microstructures indicates chancelloriids and halkieriids are closely related. *Palaeontology*, 51 (4): 865–879.

Porter, S.M. (2010). Calcite and aragonite seas and the de novo acquisition of carbonate skeletons. *Geobiology*, 8: 256–257.

Putnis, A. (2002). Mineral replacement reactions: from macroscopic observations to microscopic mechanisms. *Mineralogical Magazine*, 66: 689–708.

Runnegar, B. (1985). Shell microstructures of Cambrian molluscs replicated by phosphate. *Alcheringa: An Australian Journal of Palaenotolgy*, 9 (4): 245-257.

Runnegar, B. and P. A. Jell (1976). Australian Middle Cambrian molluscs and their bearing on early molluscan evolution. *Alcheringa: An Australian Journal of Palaenotolgy*, 1:109–138.

Runnegar, B., J. Pojeta, Jr., N.J. Morris, J.D. Taylor, and G. McClung (1975). Biology of the Hyolitha. *Lethaia*, 8: 181–191.

Russell, R. T. and N. A. Trueman (1971). The geology of the Duchess phosphate deposits, northwestern Queensland, Australia. *Economic Geology*, 66:1186–1214.

Scotese, C.R., R.K. Bambach, C. Barton, R. Van der Voo, and A.M. Ziegler (1979). Paleozoic base maps. *Journal of Geology*, 87: 217–277.

Shergold, J.H, and E.C. Druce (1980). Upper Proterozoic and Lower Palaeozoic rocks of the Georgina Basin. In *The geology and geophysics of northeastern Australia*, R.A. Henderson and P.J. Stphenson, eds, Geological Society of Australia, Inc., Brisbane, 149–174.

Shergold, J. H. and P. N. Southgate (1986). Middle Cambrian phosphatic and calcareous lithofacies along the eastern margin of the Georgina Basin, Western Queensland. Geological Society of Australia, Sydney. In *Australian Sedimentologists Group Field Guide*, series 2. Geological Society of Australia, Sydney, 89 p.

Smith, A.B. (1980). Stereom microstructure of the echinoid test. *Special Papers in Palaeontology*, 25: 1–81.

Soundry, D. and P. N. Southgate (1989). Ultrastructure of a Middle Cambrian primary nonpelletal phosphorite and its early transformation into phosphate vadoids: Georgina Basin, Australia. *Journal of Sedimentary Petrology*, 59: 53–64.

Southgate, P. N. and J. H. Shergold (1991). Application of sequence stratigraphic concepts to Middle Cambrian phosphogenesis, Georgina Basin. Australia: *Journal of Australian Geology and Geophysics*, 12: 119–144.

Southgate, P. N., J. R. Laurie, J. H. Shergold, and K. J. Armstrong (1988). Stratigraphic drilling in the Georgina Basin Burke River Structural Belt, August 1986–January 1987. *Bureau of Mineral Resources, Geology and Geophysics Record*, 1, 44 p.

Sumrall, C.D., J. Sprinkle, and T.E. Guensburg (1997). Systematics and paleoecology of Late Cambrian echinoderms from the western United States. *Journal of Palaeontology*, 71 (6): 1091–1109.

Syssoiev, V.A. (1968). [Stratigraphy and hyoliths of the oldest Lower Cambrian beds of the Siberian Platform.] *Yakutsky Filial, Sibirskoe Otdelenie, Akademii Nauk SSSR*: 1–67. [In Russian].

Ubaghs, G. and R.A. Robison (1988). Homalozoan echinoderms of the Wheeler Formation (Middle Cambrian) of western Utah. *The University of Kansas Paleontological Contributions*, Paper 120: 1–17.

Walter, M.R., J.J. Veevers, C.R. Calver, and K. GREY (1995). Neoproterozoic stratigraphy of the Centralian Superbasin. Australia: *Precambrian Research*, 73: 173–195.

Xiao, S. and J.D. Schiffbauer (2009). Microfossil phosphatization and its astrobiological implications. *In* J. Seckbach and M. Walsh (eds.), From Fossils to Astrobiology, 12, 89–117.

Zamora, S., S. Clausen, J.J. Álvaro, and A.B. Smith (2010). Pelmatozon echinoderms as colonizers of carbonate firmgrounds in mid-Cambrian high energy environments. *PALAIOS*, 25: 764–768.

Zamora, S., C.D. Sumrall, and D. Vizcaïno (2012). Morphology and Ontogeny of the Cambrian Echindoderm *Cambraster cannati* from Western Gondwanna. *Acta Palaeontologica Polonica*, 58 (3): 545–559.

Zamora, S., B. Lefebvre, J.J. Álvaro, S. Clausen,O. Elicki, O. Fatka, P. Jell, A. Kouchinsky, J. Lin, E. Nardin, R. Parsley, S. Rozhnov, J. Sprinkle, C.D. Sumrall, D. Vizcaïno, and A.B. Smith (2013). Cambrian echinoderm diversity and palaeobiogeography. *Geological Society, London, Memoirs*, *38* (1), 157–171.

Zeebe, R.E. and D. Wolf-Gladrow (2001). CO_2 in seawater: equilibrium, kinetics, isotopes. In: Halpern D (ed.), *Oceanography Series*, 65. Elsevier, Amsterdam.

Figures

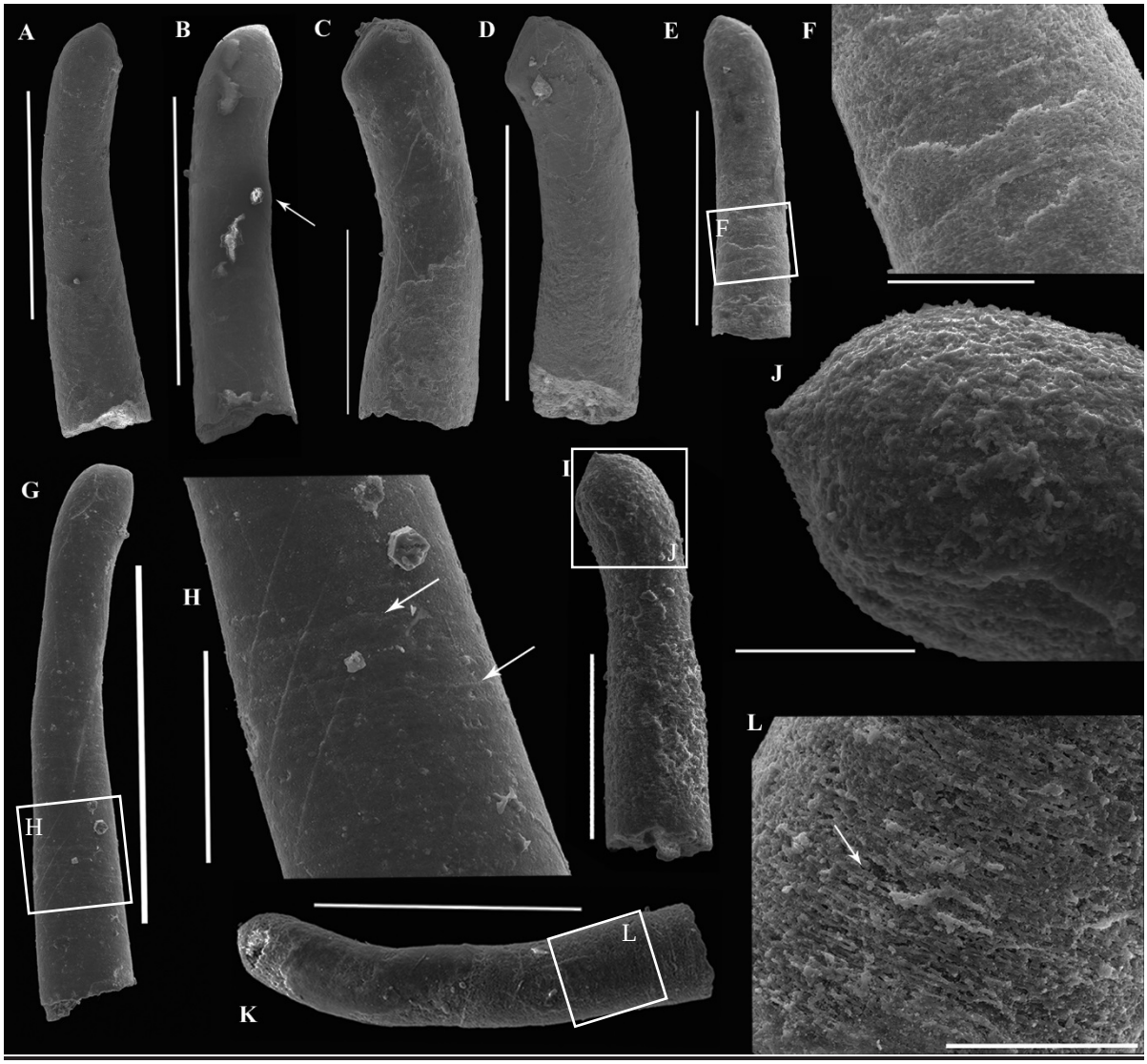

Figure 1 New hyolith species with a variety of apical shapes (angular vs. bulbous), **A.** PK98-42C11; **B.** PK98-42A21 with arrow showing irregular bulge; **C.** PK98-42A42; **D.** PK98-42C6; **E-F.** PK98-42A6, F close up of E showing fibrous microstructure; **G-H.** PK98-42A65, H showing close up of G with arrows indicating possible growth lines; **I-J.** PK98-42A9, J showing close up of I, which clearly illustrates the diagnostic ridge of *N. newspecies* as well as displays a more bulbous apex; **K-L.** PK98-42B33, L showing a close up of K, depicting the fibrous microstructure (arrow). Scales: A,D,E,K 300 μm; B 400 μm; C,I 200 μm; F,J 50 μm; G 500 μm; H 100 μm; and L 40 μm.

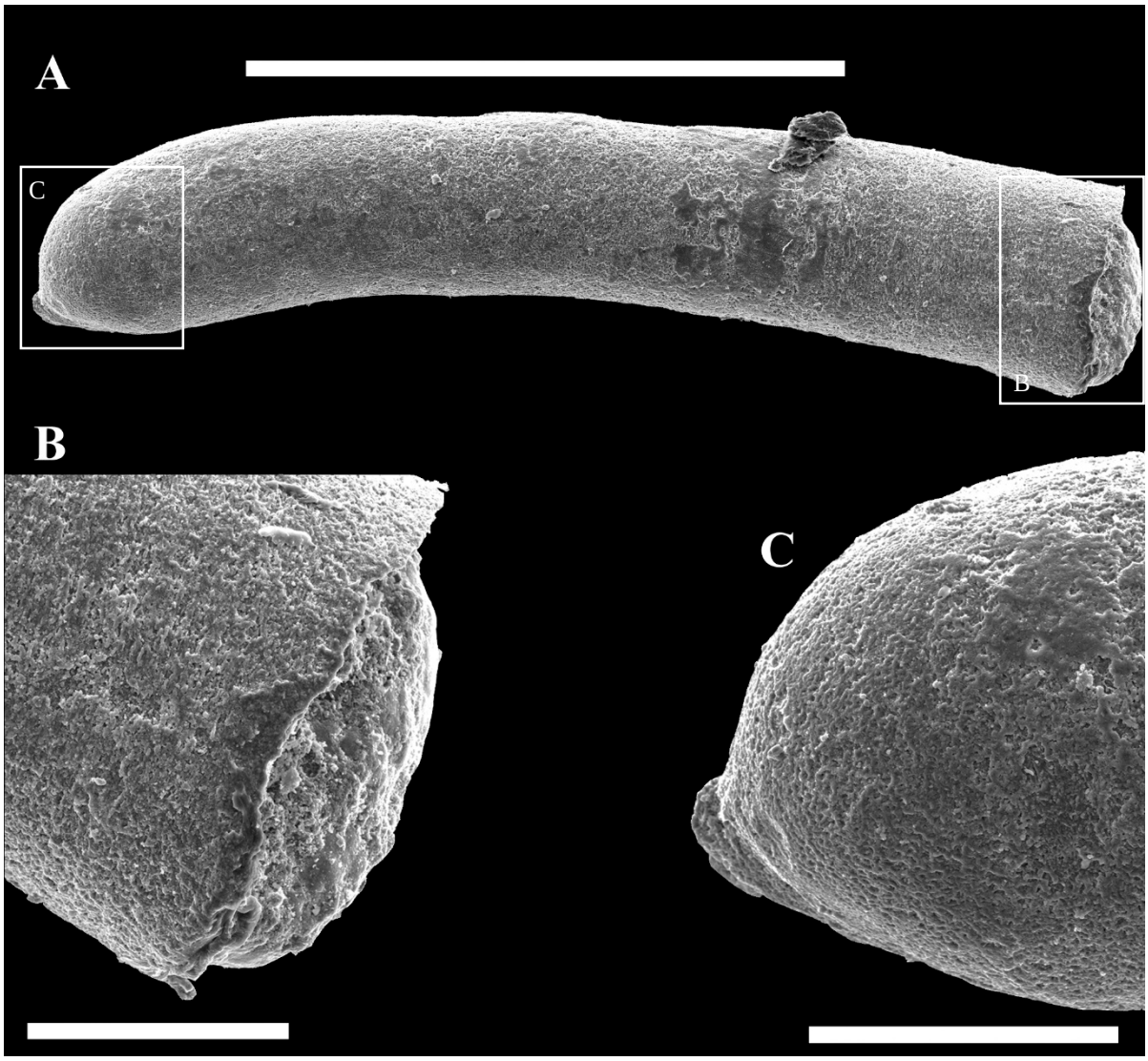

Figure 2 PK98-42A31 Holotype of a new hyolith species, showing **A.** whole specimen, **B.** flat aperture, **C.** ridged apex. Scales = 50 μm except for A, scale = 300 μm.

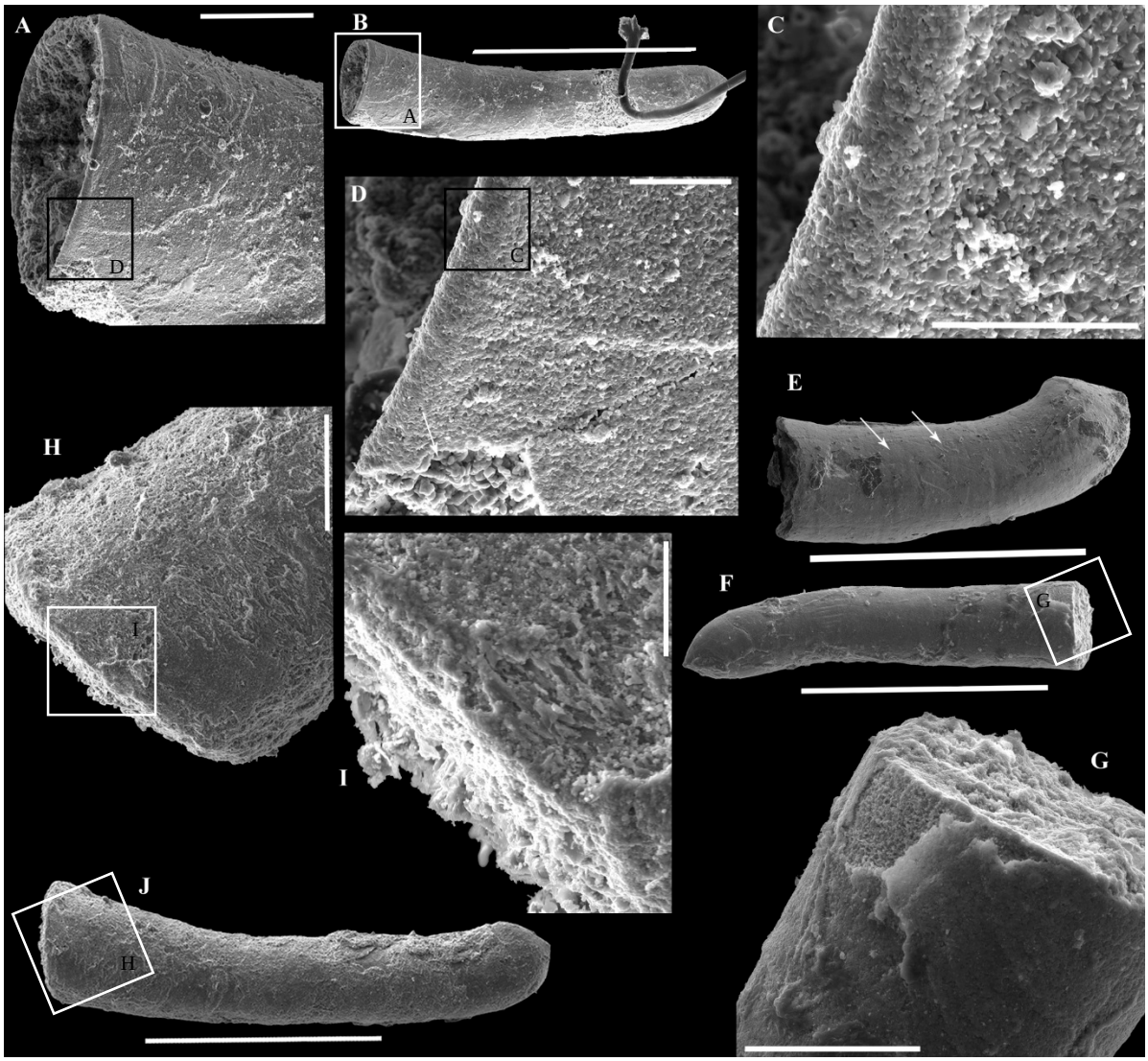

Figure 3 New hyolith species. **A-D.** PK98-48A3 with A, C, and D showing magnified views of the straight-cut, circular aperture of B; C illustrates the difference in microstructure between the apertural rim and the rest of the conch; the arrow in D shows the randomly oriented, sub-micrometric, equant apatite crystals (*cf.* Xiao and Schiffbauer, 2009: fig. 6) of the internal mold. **E.** PK98-42C4, with arrows pointing to possible growth lines on the internal mold; **F-G.** PK98-42B41, with G emphasizing the straight-cut, circular aperture of F; **H-J.** PK98-44B12, with H and J showing close-ups of the straight-cut aperture of J. Scales = 300 μm, except A,H 50 μm and C,D,I 10 μm.

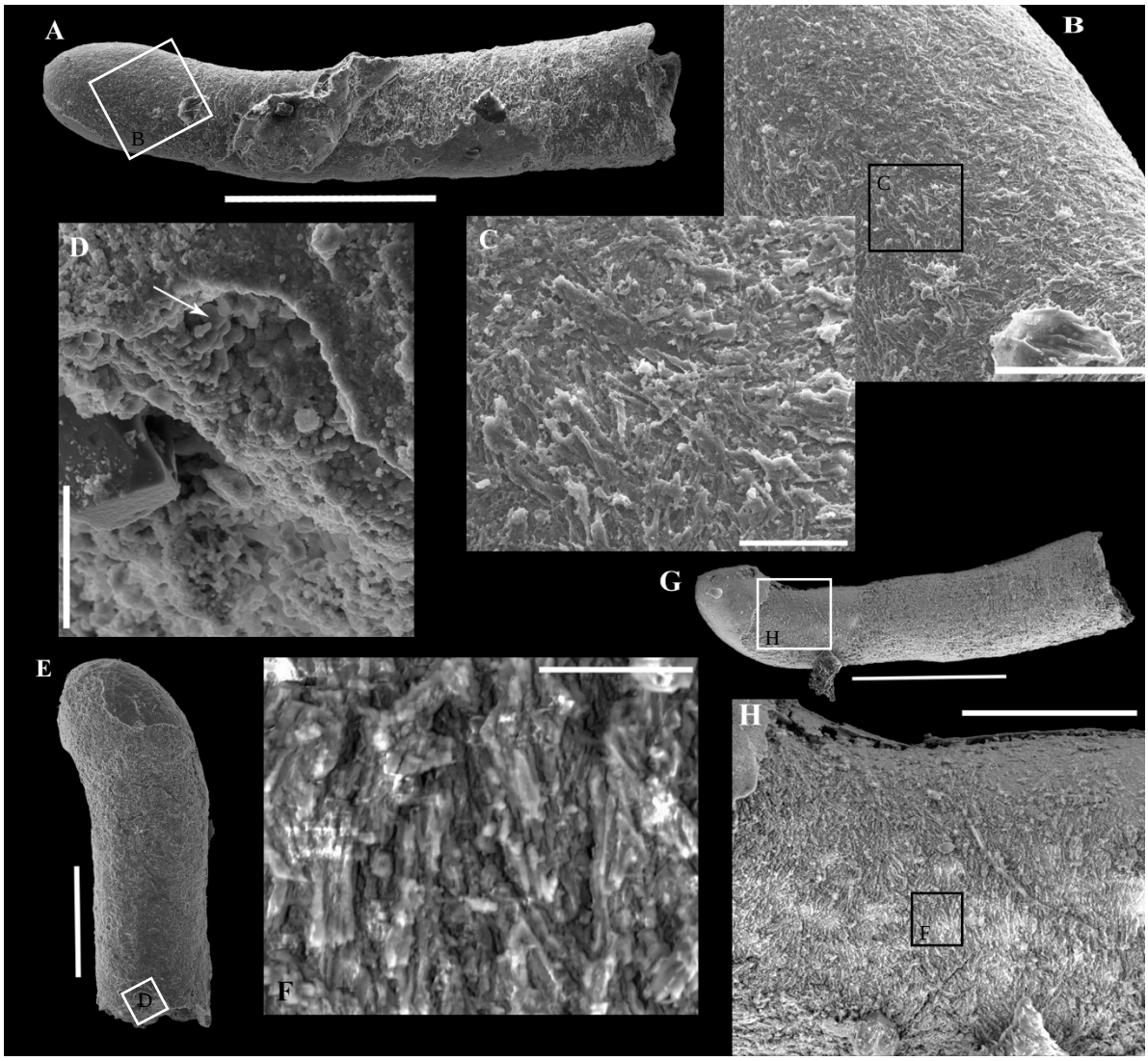

Figure 4 New hyolith species. **A-C.** PK98-397, where B and C show magnified views of the fibrous, rod-shaped structures oriented at oblique angles; **D-E.** PK98-42A28, D showing a magnified view of the broken aperture of E and the arrow pointing to randomly oriented, sub-micrometric, equant apatite crystals; **F-H.** PK98-41ag, F and H showing magnifications of the lamello-fibrillar microstructure of G. Scales: A,G 200 μm, B 40 μm, C,D,F 10 μm, E 100 μm, and H 50 μm. Photos F-H courtesy of J. Moore.

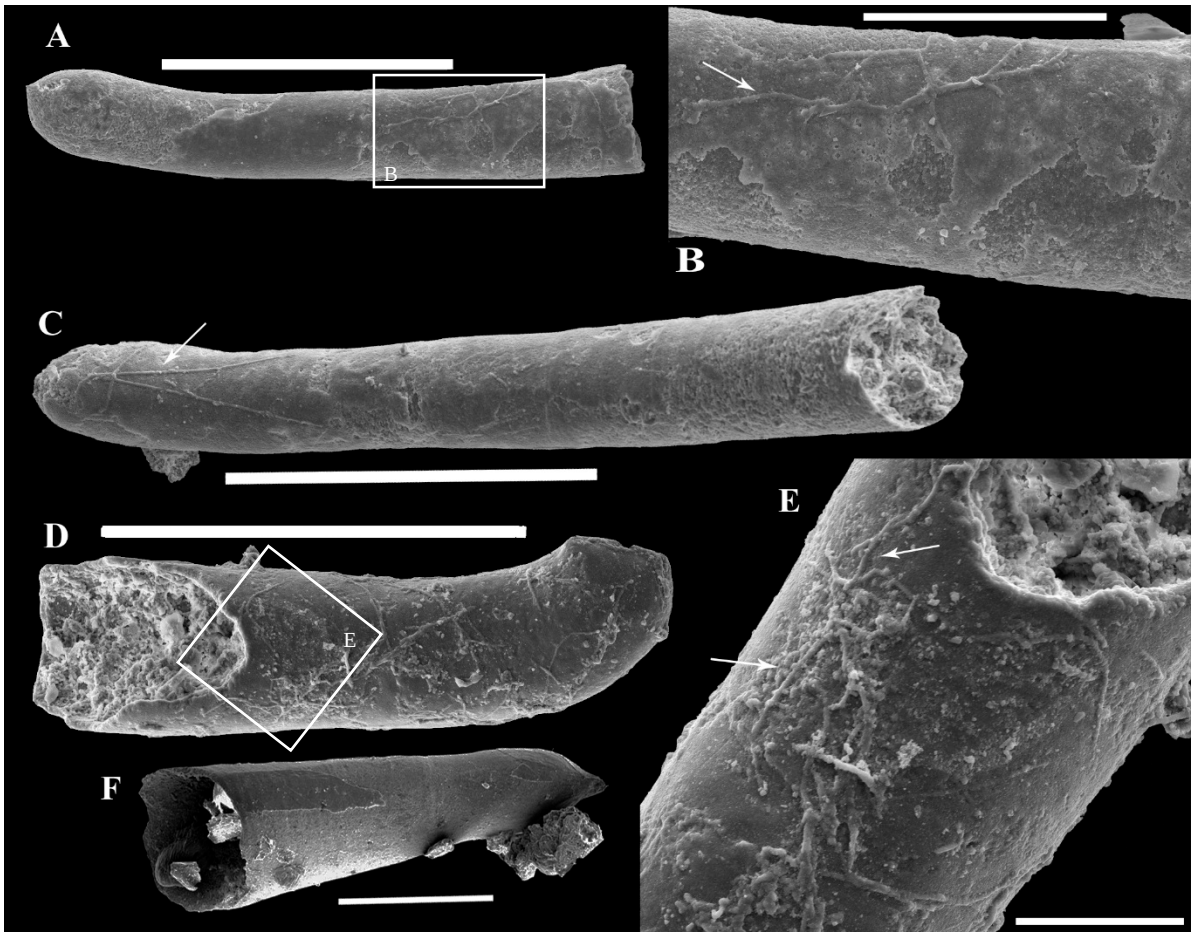

Figure 5 Cyanobacterial borings (arrows) on a new species of hyolith, **A-B.** PK98-42B8, B magnifying the borings on A; **C.** PK98-42B42; **D-E.** PK98-42B46, E showing some borings on D. **F.** Unidentified hyolith with a pointed apex. Scale = 300 μm except B 100 μm, E 50 μm, and F 200 μm.

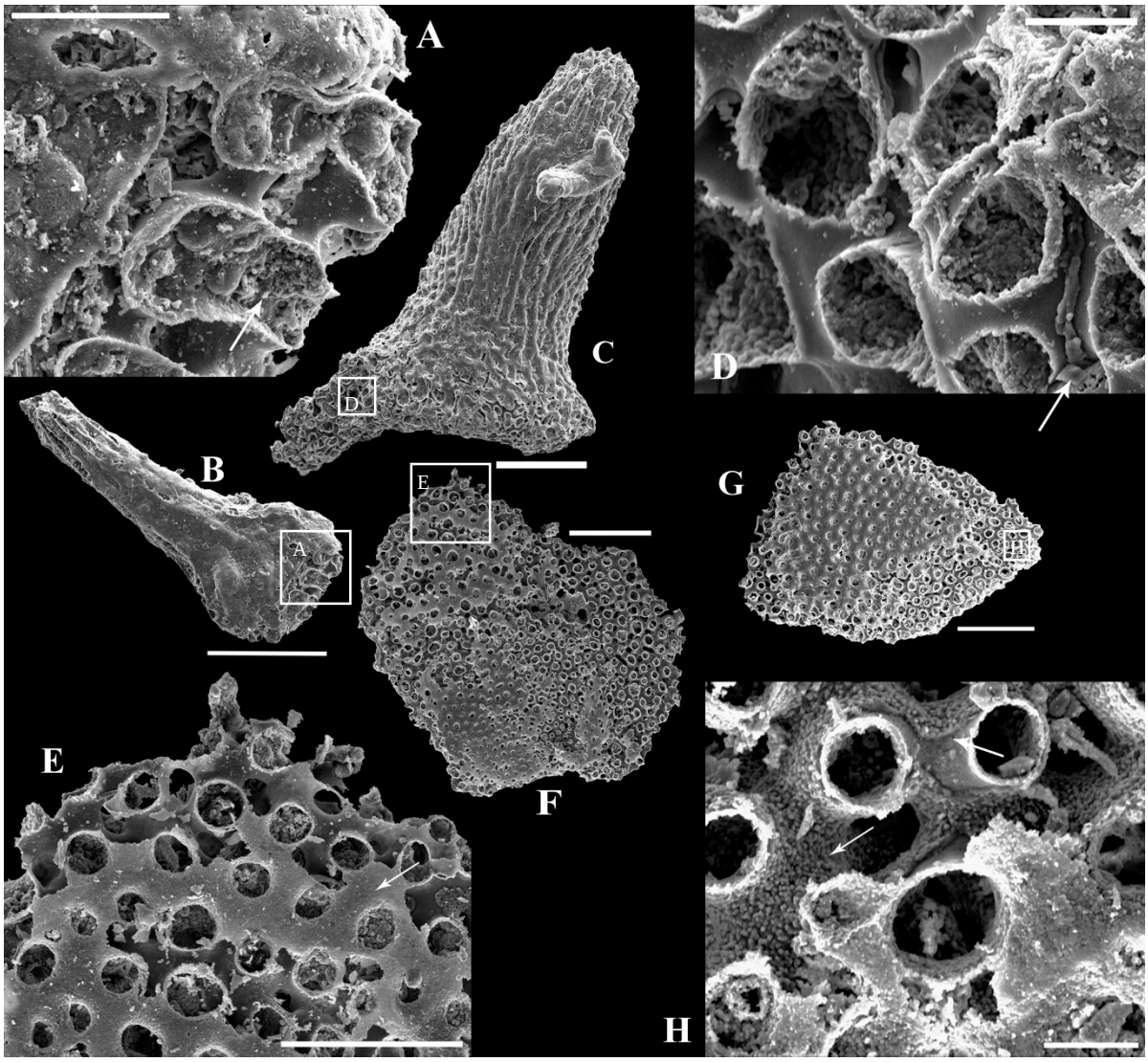

Figure 6 Echinoderm ossicles and fragments, **A-B.** PK98-41B26 fin-shaped osscile, A showing the close-up of B and arrow indicating two pores apparently fused together; **C-D.** PK98-41B38 stemmed-canal (type B, potential *Cothurncystis? bifida*) showing smooth walls where the original material contacted before maceration and an arrow pointing to diagenetic material resting on the smooth surface; **E-F.** PK98-41B44, E showing a close-up of F with an arrow pointing to diagenetic coating; **G-H.** PK98-41B12, H showing a blown-up version of G, with arrows pointing to possible replacement by apatite. Scales: A 20 μm, B,C,F 100 μm, D,H 10 μm, and E 50 μm.

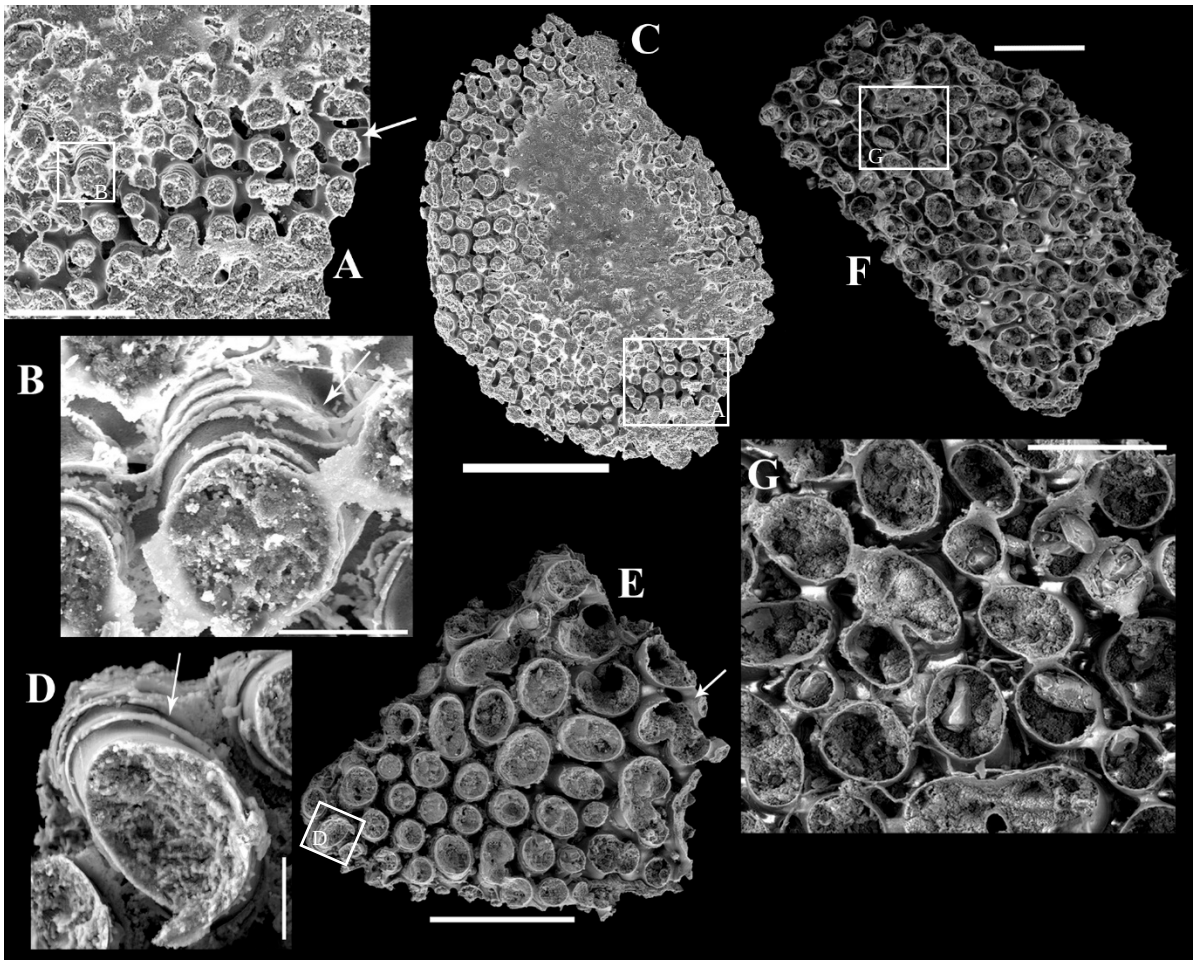

Figure 7 Echinoderm ossicles with similar microstructure to *Cantabria labyrinthica*, **A-C.** PK98-48A25, A showing a close-up of C with an arrow pointing to the smooth surface where the original trabeculae contacted, and B magnifying a pore of A with an arrow pointing to potential replacement similar to that of *C. labyrinthica* apatite layers; **D-E.** PK98-41as, potential *C. labyrinthica* with D showing layers of apatite around tubes (arrow), though the specimen still possesses smooth walls as seen in echinoderms (arrow in E); **F-G.** PK98-41an representing a potential *C. labyrinthica*. Scales: A,G 50 μm; B,D 10 μm; and C,E,F 100 μm. Photos D-G courtesy of J. Moore.

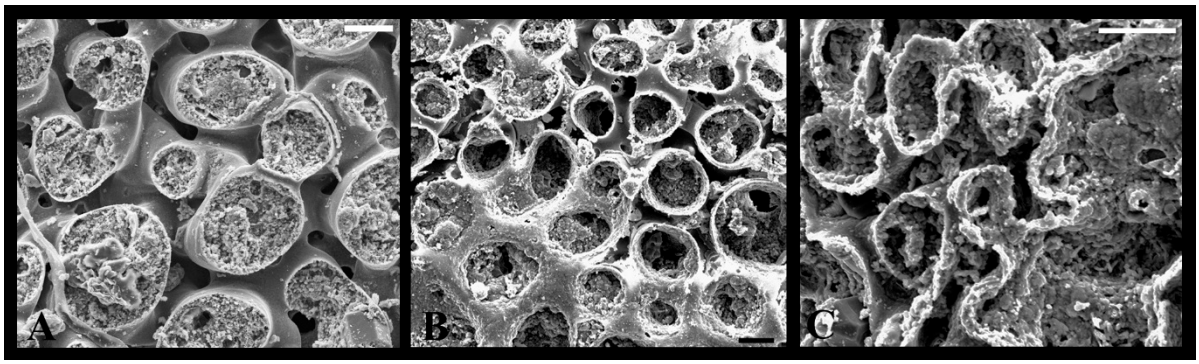

Figure 8 Microstructures of echinoderm ossicles, **A.** phosphatic mold with smooth surfaces and diagenetically-filled pores; **B.** phosphatic mold with some coating of trabecular voids; **C.** phosphatic mold with diagenetic debris. Scales = 10 μm.

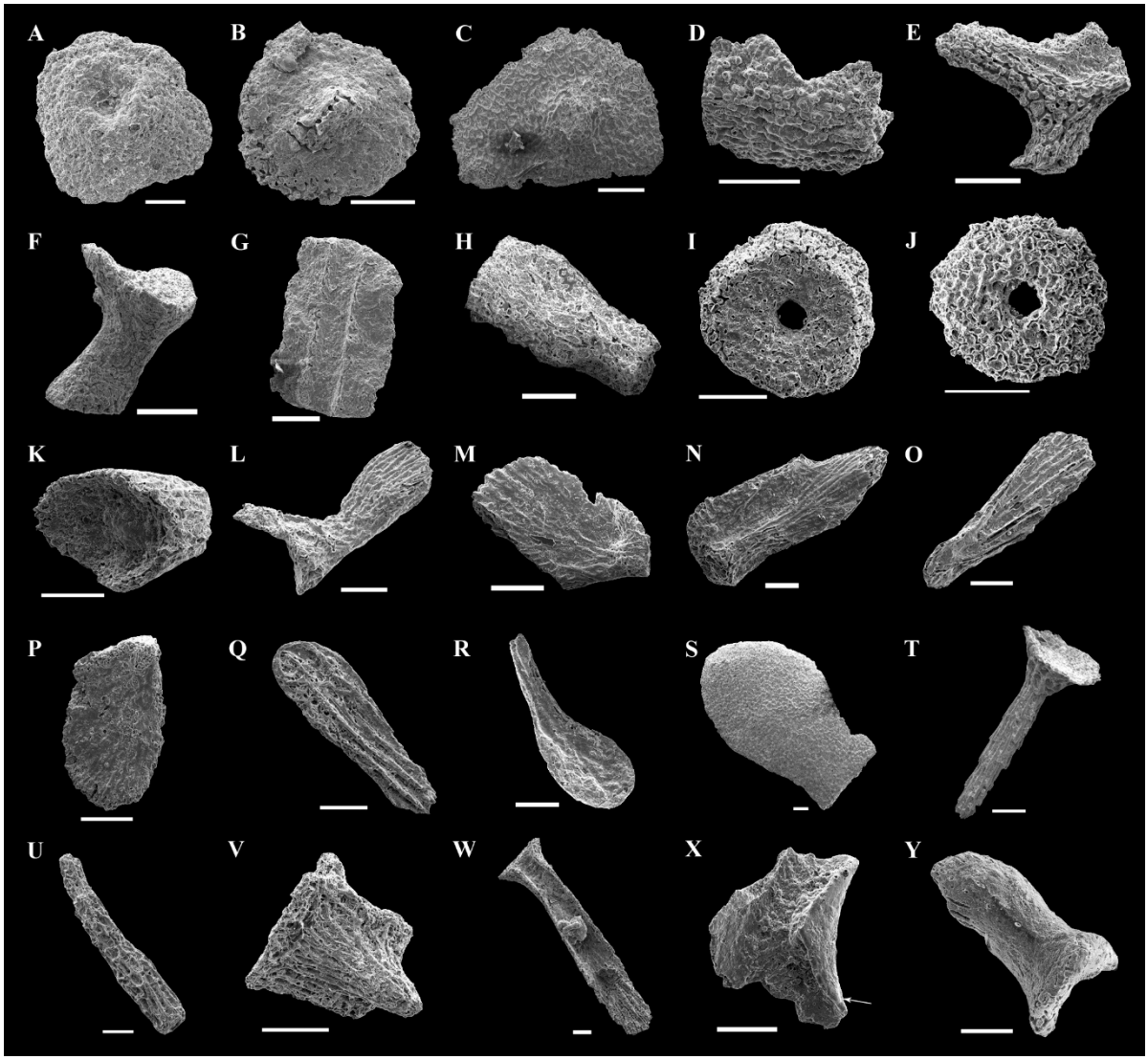

Figure 9 Echinoderm ossicle morphotypes: **A.** PK98-48A24, basal type A; **B.** PK98-44B1, basal type B; **C.** PK98-41C4, basal type C; **D.** PK98-41B17, box-shaped ossicle; **E.** PK98-41B55, branch-shaped type A; **F.** PK98-44C3, branch-shaped type B; **G.** PK98-41B49, canal; **H.** PK98-41B22, columnal(?) type A; **I.** PK98-41B10, columnal type B, possibly a discoidal holdfast (*cf.* Clausen and Peel, 2012: fig. 10f-g); **J.** PK98-41B8, columnal type B; **K.** PK98-41B28, cup-shaped ossicle; **L.** PK98-41B21, fan-shaped type A, bearing arched projection; **M.** PK98-41B61, fan-shaped type A with rounded base; **N.** PK98-41B19, fan-shaped type B; **O.** PK98-41B29, fan-shaped type C; **P.** PK98-41B42, fan-shaped type D; **Q.** PK98-41B36, fin-shaped with a wider stemming area; **R.** PK98-41B18, fin-shaped with a narrow 'stem'; **S.** PK98-44C1; petal-shaped ossicle; **T.** PK98-41A1, spine connecting to a wide base; **U.** PK98-41B39, spine with a circular concavity in its base; **V.** PK98-41B56, squared-divide ossicle; **W.** PK98-41B34, stemmed canal type A; **X.** PK98-41B62, stemmed canal type A bearing similarities to a stylophoran (arrow points to smooth edge); **Y.** PK98-44B5, stemmed canal type B, with a rounded base. All scales = 100 μm.